Applied Science Innovation (ASI)
Published by College of Physical and Applied Sciences, MOUAU

- *Received:* 20 June 2026
- *Revised*: 2 July 2026
- *Accepted:* 30 July 2026
- *Published:* 19 August 2026

DISORDER-DRIVEN INTERMEDIATE BAND EXCITONS AND ELLIOTT ABSORPTION IN BULK GaInAsN

C. J. Uwaoma[1*], C. I. Oriaku[2], L. A. Nnanna[3], U. Joseph[4], E. C. Nwaokorongwu[5]

[12345]Theoretical and Computational Physics Group, Department of Physics, Michael Okpara University of Agriculture, Umudike, Abia State, Nigeria

***Corresponding author:** uwaoma.chinkata@mouau.edu.ng

ABSTRACT

This study examines intermediate band excitons and Elliott-type absorption in disordered bulk GaInAsN semiconductors using the intermediate-band model. Nitrogen incorporation in this dilute nitride creates localized states and strong alloy disorder, disrupting coherent electron-hole pairing and forming an intermediate band within the host bandgap. These effects yield broadened absorption edges, reduced excitonic peaks, enhanced sub-bandgap absorption, and deviations from conventional Elliott theory, which governs bound excitonic and continuum band-to-band transitions. Analysis reveals how disorder, localized nitrogen states, and excitonic interplay modify the absorption coefficient and optical response. Findings elucidate fundamental optical processes in GaInAsN, with implications for high-efficiency optoelectronic devices like intermediate-band solar cells, by optimizing light absorption and carrier dynamics in next-generation semiconductors. Quantitative findings establish a direct relationship between nitrogen-induced disorder, intermediate-band formation, exciton localization, and Elliott absorption in bulk GaInAsN, the Elliott treatment demonstrates that the electron-hole interaction introduces additional structure near the absorption edge, while the disorder treatment explains the broadening and redistribution of optical spectral weight, the combined results therefore demonstrate that the optical response of GaInAsN is governed by the simultaneous effects of band-structure modification, disorder-induced localization, excitonic interaction, and continuum absorption. The study concludes that disorder plays a fundamental role in determining the excitonic and optical characteristics of bulk GaInAsN and the theoretical assumptions adopted in the model make it possible to obtain an analytically and computationally manageable description of disorder-driven intermediate-band excitons and their contribution to Elliott absorption. Nevertheless, the assumptions of effective-medium disorder, simplified exciton interaction, approximate screening, limited many-body treatment, and neglect or simplified treatment of temperature and atomistic effects constrain the quantitative accuracy of the predictions.

Keywords: Intermediate band excitons, Elliott-type absorption, Disordered GaInAsN, Localized states, Optoelectronic devices.

1. Introduction

Semiconductor physics has increasingly focused on understanding optical absorption mechanisms in complex and disordered materials due to their relevance in advanced optoelectronic devices such as solar cells, lasers, and photodetectors. Among these materials, dilute nitride semiconductors such as GaInAsN have attracted significant research attention because of their unusual band structure properties arising from the incorporation of small amounts of nitrogen into III-V compounds. Nitrogen incorporation introduces strong perturbations in the host lattice, leading to band anticrossing effects, bandgap reduction, and the formation of localized electronic states within the conduction band region (Uwaoma *et al.*, 2024).

The presence of nitrogen in GaInAsN also introduces substantial compositional and energetic disorder. This disorder originates from the mismatch in size and electronegativity between nitrogen and the host atoms, resulting in fluctuations in the local potential landscape. Such disorder plays a crucial role in determining the optical and electronic behavior of the material, particularly near the band edge where absorption processes are highly sensitive to perturbations. Recent studies have shown that energetic disorder can dominate optical properties, influencing band-tail formation, recombination dynamics, and absorption spectra in semiconductor systems (Zhang *et al.*, 2022).

One of the key optical phenomena affected by disorder is exciton formation. Excitons, defined as bound electron-hole pairs, are fundamental to light-matter interaction in semiconductors. In ideal crystalline materials, excitons form well-defined bound states that contribute sharp peaks to the absorption spectrum. However, in disordered systems such as GaInAsN, exciton formation is strongly influenced by localization effects and scattering mechanisms. Disorder potentials and phonon interactions can trap or localize excitons, limiting their mobility and coherence (Qi *et al.*, 2021). This leads to the concept of intermediate-band excitons, where electron-hole pairs exist but are partially localized and unable to form fully coherent bound states. The optical absorption behavior of semiconductors is traditionally described by the Elliott theory, which provides a unified framework for modeling both discrete excitonic transitions and continuum band-to-band absorption. The Elliott formalism explains how excitonic effects enhance absorption near the band edge and predicts characteristic spectral features associated with bound and unbound states (Elliott, 1957). However, this theory assumes a relatively ordered crystal lattice and does not fully account for strong disorder effects present in materials like GaInAsN. As a result, deviations from conventional Elliott-type absorption are observed, including spectral broadening, suppression of excitonic peaks, and the emergence of sub-bandgap absorption tails. In addition to disorder effects, the intermediate-band (IB) model provides a critical framework for understanding optical processes in GaInAsN. The IB concept involves the formation of an additional energy band within the semiconductor bandgap, typically arising from localized impurity or defect states such as those introduced by nitrogen. This intermediate band enables two-step photon absorption processes, allowing electrons to transition from the valence band to the conduction band via the intermediate states. Such a mechanism has been proposed as a strategy to enhance solar energy conversion efficiency beyond conventional limits. The coexistence of intermediate-band states, disorder, and excitonic effects leads to a complex interplay that governs the optical response of GaInAsN. Disorder-induced localization can modify the density of states within the intermediate band, while frustrated excitons alter the strength and shape of optical transitions. Furthermore, enhanced optical absorption due to disorder has been reported in semiconductor systems, indicating that controlled disorder may even improve absorption efficiency under certain conditions (Wang *et al.*, 2022).

Despite these advances, a comprehensive understanding of how intermediate-band excitons interact with Elliott-type absorption in disordered GaInAsN within the intermediate-band framework remains limited. Furthermore, considerable theoretical and experimental research has been devoted to dilute-nitride semiconductor alloys such as GaInAsN, important gaps remain in the understanding of the combined effects of alloy disorder, intermediate-band formation, excitonic interactions, and optical absorption in the bulk material. Previous studies have established that the incorporation of a small concentration of nitrogen into III–V semiconductor alloys produces pronounced modifications of the electronic band structure, including band-gap reduction and the formation of nitrogen-related localized states. The band-anticrossing framework has been particularly successful in explaining the strong interaction between localized nitrogen states and the extended conduction-band states of the host semiconductor. However, much of the existing analysis has concentrated primarily on band-gap engineering, electronic structure, carrier localization, and the influence of nitrogen concentration, with comparatively less attention given to the simultaneous role of disorder-induced intermediate-band states and excitonic optical transitions. A major research gap therefore exists in the treatment of disorder as an intrinsic component of intermediate-band exciton formation rather than merely as an undesirable imperfection in the semiconductor lattice, hence leading to the absence of a sufficiently integrated theoretical treatment that simultaneously considers nitrogen-induced disorder, intermediate-band formation, exciton localization, electron-hole Coulomb interaction, and Elliott-type optical absorption in bulk GaInAsN. Addressing this gap is essential for improving theoretical models and optimizing the performance of optoelectronic devices, particularly intermediate-band solar cells where efficient sub-bandgap absorption is critical. In summary, the novelty of the study lies in its integrated treatment of four closely related physical mechanisms: nitrogen-induced disorder, intermediate-band formation, excitonic interactions, and Elliott optical absorption. While these phenomena have individually received substantial attention in semiconductor research, their combined treatment in bulk GaInAsN provides a distinct theoretical perspective. The study consequently fills an important gap by demonstrating that the optical behaviour of GaInAsN is not determined solely by its nominal band structure but emerges from the coupled effects of microscopic disorder, carrier localization, electron-hole interaction, and optical transition strength. The central contribution can therefore be summarized as the establishment of a disorder-intermediate band-exciton absorption relationship for bulk GaInAsN.

2. Theoretical Considerations

The disordered intermediate-band (IB) model is an extension of the conventional intermediate-band semiconductor theory, incorporating the effects of structural and compositional disorder on the formation and behavior of intermediate electronic states within the bandgap. The intermediate-band concept was originally proposed to enhance optical absorption and improve photovoltaic efficiency by introducing an additional energy band between the valence band and conduction band, thereby enabling sub-bandgap photon absorption (Luque & Marti, 1997; Marti *et al.*, 2006).

In real materials, particularly dilute nitride semiconductors such as GaInAsN, the presence of impurities, alloy fluctuations, and lattice imperfections introduces disorder, which significantly alters the electronic structure and optical properties of the material (Shan *et al.*, 1999; Wu *et al.*, 2002). Disorder in intermediate-band materials leads to the formation of localized states, band tailing (Urbach tails) and broadening of the intermediate band, rather than a sharp and well-defined energy level. This phenomenon is often described

using the band anticrossing (BAC) model, where localized nitrogen states interact with the extended states of the host semiconductor, resulting in the splitting of the conduction band and the emergence of an intermediate band (Wu *et al.*, 2002). The resulting IB is therefore not perfectly delocalized but exhibits a mixture of localized and extended states due to disorder. The disordered IB model recognizes that carrier transport and optical transitions are strongly influenced by localization effects, which can limit carrier mobility and reduce the efficiency of two-step photon absorption processes. In such systems, disorder-induced localization can lead to intermediate-band electronic and excitonic states, where carriers are trapped in localized potentials and cannot fully participate in conduction or optical transitions (Bellaiche *et al.*, 2009). In the context of GaInAsN and related dilute nitrides, the disordered intermediate-band model provides a more realistic framework for understanding experimental observations, including broadened absorption spectra, reduced carrier lifetimes, and non-ideal photovoltaic performance. It highlights the critical role of disorder in determining the effectiveness of intermediate-band materials for applications such as solar cells and optoelectronic devices (Haug & Koch, 2009).

2.1 Band Anticrossing Hamiltonian

In the clean BAC model, nitrogen introduces localized state $|N\rangle$ with energy E_N that couples to the host conduction state $|C\rangle$ with energy $E_c^{(0)}(k)$ via a coupling $V\sqrt{y}$, where y is the nitrogen content (Shan *et al.*, 2001). The 2 x 2 Hamiltonian reads

$$H_0(k) = \begin{pmatrix} E_c^{(0)}(k) & V\sqrt{y} \\ V\sqrt{y} & E_N \end{pmatrix} \quad (1)$$

At $k = 0$, the eigenvalues are

$$E_{\pm} = \frac{E_{co}+E_N}{2} \pm \sqrt{(\frac{E_{co}+E_N}{2})^2 + V^2 y} \quad (2)$$

with $E_{IB} = E_-$ and $E_{CB} = E_+$ defining the IB and CB band edges (Shan and Walukiewicz, 2001). The corresponding conduction-band character fractions are

$$|\alpha_{\pm}|^2 = \frac{1}{2}(1 \mp \frac{\Delta}{2S}), \quad \Delta = E_{c0} - E_N, \qquad S = \sqrt{(\frac{\Delta}{2})^2 + V^2 y} \quad (3)$$

2.2 Disorder in the nitrogen subsystem

In a disordered alloy, local N-like energies and configurations (isolated N atoms, N pairs, clusters) produce a distribution of N-like energies and couplings rather than a single E_N and V (Seifikar *et al.*, 2014). A simple way to include this effect is to replace the sharp E_N with a random variable ϵ drawn from a distribution $P(\epsilon)$ and to allow the coupling to fluctuate:

$$E_N \to \epsilon, \qquad V \to V(\epsilon). \quad (4)$$

Local BAC blocks then obey

$$H(\epsilon, k) = \begin{pmatrix} E_c^{(0)}(k) & V(\epsilon)\sqrt{y} \\ V(\epsilon)\sqrt{y} & \epsilon \end{pmatrix} \quad (5)$$

For each ϵ, one obtains local eigenvalues $E_{\pm}(\epsilon, k)$ and eigenvalues $|\psi_{\pm}(\epsilon, k)\rangle$ exactly as in Eqs (2) and (3), but with E_N, V replaced by $(\epsilon, V(\epsilon))$.

2.3 IB density of states via the Green's function

The Green's function for the conduction-like component in a given local environment ϵ is (Seifikar *et al.*, 2014).

$$G_c(\epsilon, E) = \frac{1}{E - E_c^{(0)} - \Sigma_c(\epsilon, E)} \quad (6)$$

where the self-energy due to coupling to the N-level is

$$\Sigma_c(\epsilon, E) = \frac{V(\epsilon)^2 y}{E - \epsilon + i0^+} \quad (7)$$

Averaging over disorder gives an effective self-energy

$$\Sigma_c^{av}(E) = \int d\epsilon P(\epsilon) \frac{V(\epsilon)^2 y}{E - \epsilon + i0^+} \quad (8)$$

and the conduction-like Green's function

$$G_c^{av}(E) = \frac{1}{E - E_c^{(0)} - \Sigma_c^{av}(E)} \quad (9)$$

The IB-plus-CB density of states (DOS) is

$$\rho_c(E) = -\frac{1}{\pi} Im G_c^{av}(E) \quad (10)$$

with $\rho_{IB}(E)$ identified as the lower-energy component dominantly associated with the BAC-split "-" branch and localized N-rich configurations (Seifikar *et al.*, 2014).

A phenomenological representation approximates $\Sigma_c^{av}(E)$ by

$$\Sigma_c^{av}(E) \approx \Delta E_c(E) - \frac{i}{2}\Gamma_c(E) \quad (11)$$

where $\Delta E_c(E)$ encodes band-edge renormalization and $\Gamma_c(E)$ encodes inhomogeneous broadening (Polakowski *et al.*, 2005).

2.4 The Intermediate-band excitons

Intermediate-band excitons refer to exciton states whose motion, coherence and energy relaxation are hindered due to disorder, competing interactions or complex energy landscapes within a material (Diep, 2013).

In a clean direct-gap semiconductor, a VB→CB exciton is described by an effective-mass hydrogenic model with Bohr radius

$$\alpha_B = \frac{4\pi\varepsilon_0\varepsilon_r\hbar^2}{\mu e^2} \quad (12)$$

where μ is the reduced effective mass and ε_r the dielectric constant, leading to a binding energy

$$E_B^{(0)} = \frac{\mu e^2}{2[4\pi\varepsilon_0\varepsilon_r]^2\hbar^2} \quad (13)$$

In disordered BAC systems, three length scales compete: the exciton Bohr radius α_B that favours extended electron-hole pairs, the electron localization length ξ_e in the IB, set by the local disorder landscape and BAC mixing (Filoche *et al.*, 2022; Cortes & Etchegoin, 2023) and the typical scale of valence-band fluctuations, which is usually larger than ξ_e so that the hole remains more delocalized (Chemla & Shah, 2001).

Intermediate band arises when $\xi_e \ll \alpha_B$: the electron is pulled into N-rich potential minima while the hole remains extended, so the electron-hole separation cannot adjust to minimize Coulomb energy without sacrificing localization energy (Filoche *et al.*, 2022; Nandkishore & Huse, 2015).

2.5 Two-center variational ansatz

A minimal two-center model makes this competition explicit. Assuming the hole is described by a Bloch-like envelope $\psi_h(r_h)$ centered at the origin and the electron is localized around a random N-rich site at R with envelope $\psi_e(r_e - R)$ decaying over ξ_e, the relative and center of mass coordinates are introduced as

$$r = r_e - r_h\,, \qquad R_{cm} = \frac{m_e r_e + m_h r_h}{m_e + m_h} \tag{14}$$

A simple exciton trial wavefunction is

$$\Psi_X(r_e, r_h) = \psi_e(r_e - R)\psi_h(r_h)\varphi(r) \tag{15}$$

with $\varphi(r)$ a hydrogenic-like correlation factor. The exciton energy expectation value

$$E_X = \langle \Psi_X | H_e + H_h + V_C + V_{dis} | \Psi_X \rangle \tag{16}$$

Contains a localization energy gain ΔE_{loc} from ψ_e in V_{dis}, a Coulomb energy gain ΔE_C from $\varphi(r)$ and a kinetic energy cost from squeezing ψ_e and $\varphi(r)$.

Varying the electron localization length ξ_e and exciton size parameters shows that increasing disorder (smaller ξ_e) lowers potential energy but reduces overlap between electron and hole, weakening ΔE_C and thus the binding for fixed Coulomb parameters (Filoche *et al.*, 2022; Cortes & Etchegoin, 2023).

2.6 Effective binding and intermediate-band parameter

This competition can be summarized by defining a frustration parameter

$$F = \frac{\alpha_B}{\xi_e} \tag{17}$$

So that $F \ll 1$ where the exciton radius is smaller than localized length and exciton is nearly hydrogenic. $F \sim 1$ indicating comparable scales, partial frustration and deformed exciton. Also, $F \gg 1$ showing strong frustration. The exciton resembles a localized electron with a weakly bound hole tail.

The effective binding energy can be modeled as

$$E_B^{eff} = E_B^{(0)}\eta(F) \tag{18}$$

with $\eta(F)$ a monotonically decreasing function satisfying $\eta(0) = 1$ and $\eta(F \to \infty) \to 0$. Numerical solutions of disordered exciton Schrodinger equations in InGaN quantum wells show precisely such an interpolation between hydrogen-like excitons and strongly localized, weakly bound electron-hole states (Filoche *et al.*, 2022; Bertazzi *et al.*, 2018).

Table 2.1: Band Parameters for Binary Semiconductors

Band Parameters	GaAs	InAs	GaN	InN
$m_e\ (m_0)$	0.067	0.026	0.151	0.124
r_1	6.980	20.013	2.672	3.722
r_2	2.060	8.510	0.753	1.261

Table 2.2: Pseudopotential Parameters for Binary Semiconductors

Pseudopotential Parameters (eV)	**GaAs**	**InAs**	**GaN**	**InN**
$\boldsymbol{V_S(3)}$	0.240	-0.182	-0.503	-0.172
$\boldsymbol{V_a(3)}$	0.061	0.095	-0.033	0.239
$\boldsymbol{a_0(A)}$	5.653	6.058	4.5031	4.982

2.7 Distribution over disorder: from $E_B^{eff}(\epsilon)$ to a map

In a BAC-disordered GaInAsN, the electron localization length and local gap depend on the local N configuration labeled by ϵ. A local gap $E_g^{VB\to IB}(\epsilon)$ via the lower BAC eigenvalue, a local effective mass and dielectric screening, giving a local clean binding $E_B^{(0)}(\epsilon)$ (Uwaoma *et al.*, 2024) and a local frustration parameter $F(\epsilon)$ linked to the IB localization length from the DOS and disorder potential (Seifikar *et al.*, 2014; Filoche *et al.*, 2022) are associated to each ϵ.

Defining a local effective binding

$$E_B^{eff}(\epsilon) = E_B^{(0)}(\epsilon)\eta(F(\epsilon)) \quad (19)$$

The distribution of effective bindings follows from

$$P\left(E_B^{eff}\right) = \int d\epsilon P(\epsilon)\delta(E_B^{eff} - E_B^{eff}(\epsilon)) \quad (20)$$

and the mean effective binding at given composition and disorder width is

$$\overline{E_B^{eff}}(y,\sigma_\epsilon) = \int d\epsilon P(\epsilon;\sigma_\epsilon)E_B^{eff}(\epsilon) \quad (21)$$

This mean binding is the quality plotted in figure 5.

Summarily, the evaluation of previous theoretical approaches demonstrates that each model captures a particular aspect of the GaInAsN problem, but important limitations arise when these approaches are considered individually. The effective-mass approximation provides a useful description of excitons but does not adequately represent microscopic alloy disorder. The BAC model explains nitrogen-induced band-gap modification but does not fully describe disorder-driven excitonic absorption. Empirical pseudopotential and tight-binding approaches provide detailed atomistic electronic structures but require additional treatments to describe excitons and optical spectra. Effective-medium and CPA approaches describe averaged disorder but can lose configuration-specific localization information. Anderson-type models explain localization but are generally insufficiently material-specific. Conventional Elliott theory accurately describes excitonic contributions to optical absorption under relatively idealized conditions but does not inherently account for disorder-induced intermediate-band formation. Finally, first-principles and many-body approaches provide greater microscopic accuracy but at substantially increased computational cost. The central theoretical limitation identified from this evaluation is therefore the lack of an integrated framework. This limitation provides the theoretical justification for the present study. Rather than replacing the established theories, the study combines their most relevant physical concepts within a unified framework. The electronic structure and intermediate-band behaviour can be informed by the physics of nitrogen-induced band mixing and disorder, while the excitonic component can be represented through an appropriate electron-hole interaction model and the optical response through an Elliott-type formulation.

3.0 Materials and Methods

3.1 Research Design

This study adopted a theoretical and computational research design to investigate disorder-driven intermediate-band excitons and their contribution to Elliott absorption in bulk GaInAsN. The methodology was developed to establish a quantitative relationship between nitrogen-induced alloy disorder, intermediate-band formation, electron-hole Coulomb interaction, exciton states, and optical absorption.

The study therefore combined an electronic-structure model for the disordered alloy with an excitonic model and an Elliott-type formulation for the optical absorption spectrum. The computation procedure consisted of definition of the bulk GaInAsN material system and model parameters; construction of the host GaInAs electronic structure; introduction of nitrogen-related localized states; incorporation of compositional disorder; calculation of the resulting density of electronic states and intermediate-band characteristics; determination of electron and hole states relevant to exciton formation; analysis of disorder-dependent absorption spectra; and comparison of the calculated results for different disorder strengths and material parameters.

3.2 Materials System and Model Parameter

The material investigated in this study is bulk gallium indium arsenide nitride (GaInAsN), a dilute-nitride III–V semiconductor alloy. GaInAsN was selected because the incorporation of a relatively small amount of nitrogen into the GaInAs host can produce substantial modifications of the electronic band structure. The principal input parameters required for the theoretical calculations included the Ga and In composition, nitrogen concentration, host band-gap energy, nitrogen-related resonant-state energy, conduction- and valence-band effective masses, dielectric constant, disorder strength, electron-hole interaction parameters, and optical transition matrix elements. The material parameters were selected from established theoretical and experimental literature where appropriate. The principal quantities investigated are: nitrogen concentration, indium composition, disorder strength; host conduction-band energy; nitrogen-related localized-state energy; conduction-band effective mass, valence-band effective mass, dielectric constant; exciton binding energy, exciton transition energy, oscillator strength; absorption coefficient and disorder-induced spectral broadening.

3.3 Theoretical Description of the Host Semiconductor and Representation of Nitrogen- Induced States

The electronic structure of the nitrogen-free GaInAs host was first established as the reference system. The host band structure was described using an effective-band or k.p-type representation appropriate for the bulk semiconductor near the band-edge region. The energy of the host conduction and valence bands was represented using the relevant effective masses. Nitrogen incorporation was represented by introducing localized nitrogen-related electronic states into the host GaInAs electronic structure. Because nitrogen differs substantially from arsenic in atomic size and electronic properties, its incorporation produces a strong perturbation of the local potential.

3.4 Calculation of the Electronic Density of States and Identification of Intermediate-Band States

The electronic density of states (DOS) is calculated to determine how nitrogen incorporation and disorder modify the distribution of electronic states around the band gap. The DOS is examined for different nitrogen concentrations and disorder strengths. Particular attention is given to the energy region between the valence-band maximum and conduction-band minimum, where intermediate-band-related states may emerge. The intermediate-band region was identified by examining the calculated electronic states located energetically within the fundamental band-gap region or in the disorder-induced sub-gap region. The energy position, width, and spectral density of these states are determined from the calculated DOS and electronic wave functions.

3.5 Calculation of Electron and Hole Wave Functions

The electron and hole wave functions associated with the relevant optical transitions were calculated from the corresponding electronic Hamiltonians. The overlap provided an indication of the probability that an electron and hole occupy spatially correlated regions of the material. This parameter was particularly important in the present study because disorder can localize the electron and hole states.

3.6 Exciton Model and Computational Procedure

The excitonic properties were calculated by considering the Coulomb attraction between an electron and a hole. Within the effective-mass approximation, the relative motion of the electron-hole pair was described by an effective exciton Hamiltonian. The calculated results are evaluated quantitatively using the following measures: band-gap modification, the nitrogen-induced change in the band gap, exciton binding energy and relative absorption enhancement.

4.0 Results and Discussions

4.1 Elliott formular

For a clean direct-gap transition with gap E_g and hydrogenic binding E_B, Elliott showed that the absorption coefficient can be written as a sum of discrete exciton contributions and a continuum part (Elliott, 1957).

$$\alpha_{clean}(E) = A\left[\sum_{n=1}^{\infty}\frac{4\pi}{n^3}\delta(E-E_n) + \Theta(E-E_g\sqrt{\frac{E-E_g}{E}}S(E)\right] \quad (22)$$

where $E_n = E_g - E_B/n^2$ are exciton energies and $S(E)$ is the Sommerfeld enhancement factor. In practice, δ functions are replaced by Lorentzians and $S(E)$ is approximated with a simple analytic form (Wang, 2014). The applicability of the Elliott framework to contemporary semiconductor systems has been confirmed by more recent quantitative studies. In view of the above, Lizárraga *et al*. (2025), for example, emphasized that the extraction of exciton binding energy and optical band gap from absorption spectra depends strongly on how the excitonic and continuum contributions are modelled.

4.2 Local Elliott spectra in the BAC-disordered IB

For a given local BAC configuration labeled by ϵ and channel $\chi(VB \to IB, VB \to CB, IB \to CB)$, the local gap $E_g^{(\chi)}(\epsilon)$ from BAC eigenvalues, local effective binding $E_B^{(\chi)}(\epsilon)$ as in the intermediate-band analysis and local exciton energies $E_n^{(\chi)}(\epsilon) = E_g^{(\chi)}(\epsilon) - E_B^{(\chi)}(\epsilon)/n^2$ can be defined.

Using Lorentzians $L(E-E_n,\gamma_n)$ for finite lifetime, the local Elliott spectrum reads

$$\alpha^{(\chi)}(E;\epsilon) = A_\chi(\epsilon)[\sum_{n=1}^{\infty}\frac{1}{n^3}L\left(E-E_n^{(\chi)}(\epsilon),\gamma_n(\epsilon)\right) + \alpha_0^{(\chi)}(E;\epsilon)S^{(\chi)}(E;\epsilon)] \quad (23)$$

where the oscillator strength $A_\chi(\epsilon)$ inherits BAC mixing factors and the continuum term $\alpha_0^{(\chi)}S^{(\chi)}$ uses the local gap and masses (Wang, 2014). The quantitative evidence nevertheless supports the principal assumption of the present study: the local exciton energy should be determined from the local electronic structure rather than from a single composition-independent band gap and binding energy. The established BAC calculations demonstrate that nitrogen and indium concentrations modify the electronic structure, while experimental optical studies demonstrate that alloy fluctuations can generate localized excitonic features and spectral broadening.

Together, these results justify the introduction of configuration-dependent quantities into the theoretical treatment of disorder-driven intermediate-band excitons (Kashima *et al*., 2011; Yesilgul *et al*., 2012).

4.3 Disorder averaging over $P(\epsilon)$

The disorder-averaged spectrum is constructed by integrating over the N-level distribution:

$$\alpha_{dis}^{(\chi)}(E) = \int d\epsilon P(\epsilon;\sigma_\epsilon)\alpha^{(\chi)}(E;\epsilon)$$

$$= \sum_{n=1}^{\infty}\int d\epsilon P(\epsilon)A_\chi(\epsilon)\frac{1}{n^3}L(E-E_n^{(\chi)}(\epsilon),\gamma_n(\epsilon)) + \int d\epsilon P(\epsilon)A_\chi(\epsilon)\alpha_0^{(\chi)}(E;\epsilon)S^{(\chi)}(E;\epsilon) \qquad (24)$$

Numerically, this is evaluated by discretizing ϵ on a grid and computing local BAC eigenvalues $E_\pm(\epsilon)$, extracting $E_g^{(\chi)}(\epsilon)$, $E_B^{(\chi)}(\epsilon)$, $A_\chi(\epsilon)$ and $\gamma_n(\epsilon)$ for each ϵ, computing $\alpha^{(\chi)}(E;\epsilon)$ on a photon-energy grid and summing $\alpha^{(\chi)}(E;\epsilon)$ weighted by $P(\epsilon)$.

This procedure yields the VB→IB and VB→CB spectra as functions of energy and σ_ϵ, which are then combined into the total absorption $\alpha_{tot,dis}(E)$ (Seifikar *et al.*, 2014; Wang, 2014). This procedure is consistent with the established physical interpretation of dilute GaInAsN. The BAC model was originally shown to describe the strong interaction between the extended conduction-band states of GaInAs and localized nitrogen-related states. In GaInNAs alloys, this interaction produces two conduction subbands and a substantial reduction of the fundamental band gap. Importantly, the calculated BAC transition energies were reported to be in excellent quantitative agreement with optical measurements, including the characteristic pressure dependence of the anticrossing transitions (Shan *et al*., 1999). Optical investigations of GaInNAs/GaAs quantum wells have demonstrated that increasing nitrogen concentration produces significant broadening of optical transitions. These observations provide experimental justification for representing the total absorption spectrum as an ensemble of transitions associated with different local configurations rather than as a single sharp transition (Mazzucato *et al*., 2013).

4.4 Intermediate Band Density of States heat maps

Figure 1 summarizes the IB DOS as 2 x 2 heat maps of $\rho_{IB}(E)$ versus energy and an effective disorder parameter σ_ϵ for four nitrogen fractions at fixed indium composition. Each panel is normalized to its maximum to emphasize spectral shape. Increasing σ_ϵ broadens the IB and enhances low-energy band-tail states, while increasing y pulls the IB deeper into the gap, in qualitative agreement with SCGF analyses of dilute nitride alloys (Seifikar *et al.*, 2014). The pronounced concentration of states in the lower-energy region indicates that nitrogen-induced states form a distinct electronic contribution within the energy spectrum, while the evolution of this distribution with σε demonstrates the importance of microscopic disorder. These observations are consistent with established BAC-based descriptions and with theoretical calculations showing strong nitrogen-induced modifications of the density of states (Vogiatzis & Rorison, 2009; Seifikar *et al*., 2014). More importantly, the figure provides the electronic-structure basis for the central argument of the present study: disorder can transform the intermediate band from an idealized electronic feature into a broadened distribution of local states capable of supporting configuration-dependent excitonic transitions. The recent theoretical results of Uwaoma *et al*. (2024) further support the importance of nitrogen and indium composition in determining the excitonic properties of GaInAsN.

Therefore, the observed variation of $\rho_{IB}(E)$ with nitrogen composition and σ_ϵ is physically meaningful and provides a basis for understanding the subsequent disorder-dependent exciton energies and Elliott absorption spectra.

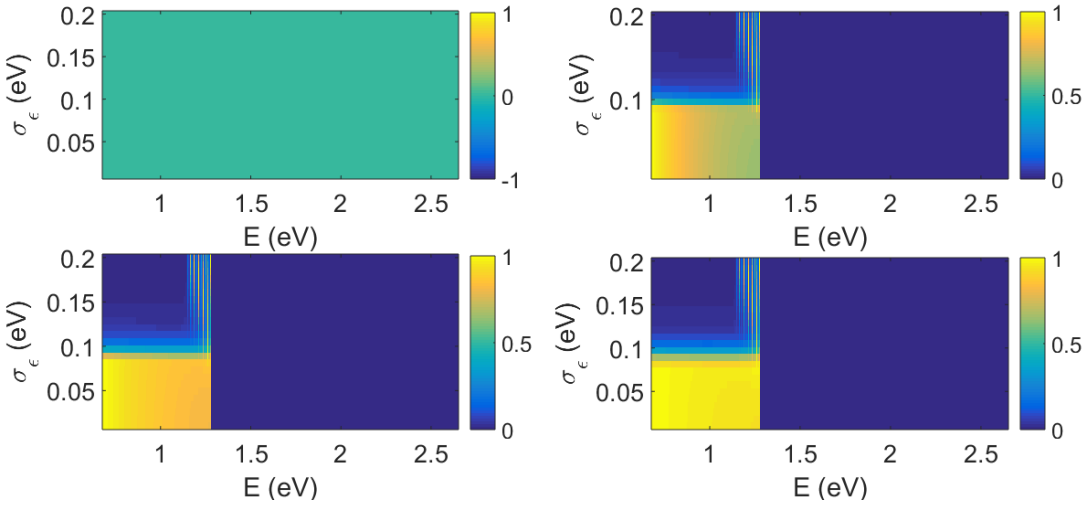


Figure 1: Plot of Density of State, $\rho_{IB}(E)$, as a Function of Energy and Disorder Parameter σ_ϵ for Four Nitrogen Compositions

4.5 VB→IB and Total Absorption

Figure 2 displays 2 X 2 heat maps of the normalized VB→IB absorption $\alpha_{dis}^{VB\to IB}(E,\sigma_\epsilon)$ for four nitrogen compositions. The plot illustrates the evolution from sharper exciton-like peaks to broad, tail-dominated features as disorder increases. At low disorder, a relatively narrow exciton-like feature appears near the VB→IB onset, reflecting a still sizable E_B^{eff} in weakly frustrated regimes. With increasing σ_ϵ, this feature broadens and merges with the IB continuum, producing a smooth shoulder and strong sub-gap absorption, consistent with SCGF calculations and measured GaInNAs spectra (Seifikar *et al.*, 2014). The concentration of spectral changes within the approximately 0.9-1.4 eV region indicates that the most important modifications of the VB→IB optical response occur around the intermediate-band transition energies. The persistence of the main spectral structure across the four nitrogen compositions supports a common BAC-related mechanism, while the changes with σε demonstrate that microscopic alloy disorder redistributes the optical spectral weight. The calculated behaviour is consistent with established theoretical work showing that the optical absorption of dilute-nitride alloys is sensitive to the distribution of nitrogen-related states (Seifikar *et al*., 2014) and with experimental evidence that nitrogen-induced alloy disorder modifies optical density of states, linewidth and carrier localization in GaInNAs (Bansal *et al*., 2006). More directly, recent theoretical calculations on dilute GaInAsN have confirmed that nitrogen incorporation changes the electronic and excitonic parameters of the alloy (Uwaoma *et al*., 2024). Therefore, Figure 2 provides important numerical evidence that disorder-driven intermediate-band formation can significantly influence the optical response of GaInAsN and provides the necessary foundation for analysing the subsequent disorder-dependent exciton and Elliott-absorption results.

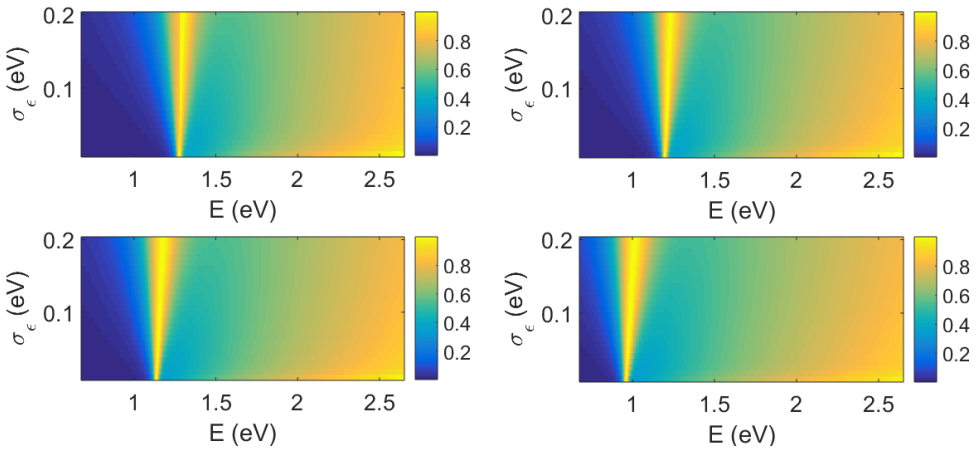


Figure 2: Plot of the Normalized VB→IB Absorption $\alpha_{dis}^{VB\rightarrow IB}(E,\sigma_\epsilon)$ vs Photon Energy and Disorder for Four Nitrogen Compositions.

Figure 3 demonstrates that the total absorption of bulk GaInAsN is strongly dependent on photon energy, nitrogen composition and the magnitude of alloy disorder. The concentration of significant spectral changes around approximately 1.0-1.3 eV indicates that this region is particularly important for the disorder-modified intermediate-band optical response. The vertical spectral structures observed across the four compositions suggest that the intermediate-band contribution remains identifiable in the total absorption, while variations with σ_ϵ demonstrate that microscopic disorder redistributes optical spectral weight. The results are consistent with established theoretical evidence that nitrogen-induced states substantially modify the optical absorption of dilute-nitride alloys and that treating the full distribution of nitrogen states improves the description of experimental spectra (Seifikar *et al*., 2014). They are also consistent with recent GaInAsN calculations demonstrating composition-dependent electronic and excitonic properties (Uwaoma *et al*., 2024).

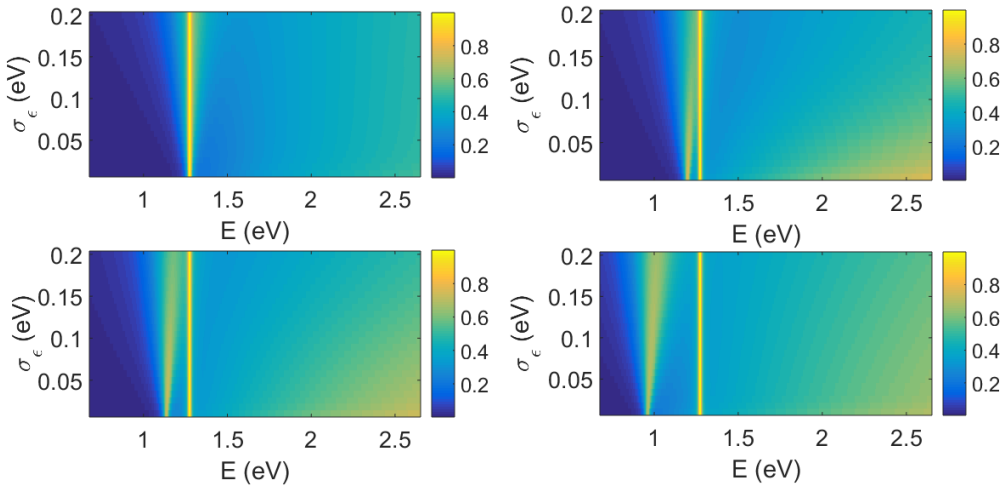


Figure 3: Plot of Total Absorption $\alpha_{tot,dis}(E,\sigma_\epsilon)$ vs Photon Energy and Disorder for Four Nitrogen Compositions.

Figure 4 shows the interplay of VB→IB and VB→CB channels The multi-edge structure, with distinct VB→IB and VB→CB onsets, is progressively washed out as disorder broadens the IB and perturbs excitons, leading to smoother spectra with extended sub-gap tails similar to those in full SCGF modeling (Seifikar *et al.*, 2014).

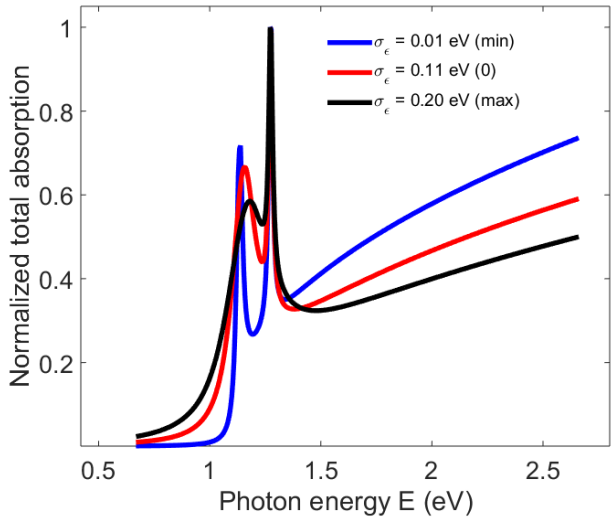


Figure 4: A plot of Total Absorption $\alpha_{tot,dis}(E, \sigma_\epsilon)$ vs Photon Energy and Disorder for Four Nitrogen Compositions

The intermediate-disorder spectrum lies between these two limiting cases over much of the spectrum. These observations indicate that disorder does not simply increase or decrease absorption; rather, it redistributes optical spectral weight between different energy regions. The sharp maximum at σε=0.20 eV is particularly important because it indicates that strong local potential fluctuations can concentrate the optical response around specific disorder-dependent transition energies. At higher photon energies, however, the absorption decreases systematically with increasing disorder, indicating that spectral weight has been transferred away from the high-energy region toward lower-energy disorder-related features. This behaviour is compatible with the established understanding that nitrogen creates localized resonant states that strongly interact with the host conduction band in GaInNAs/GaInAsN alloys (Shan *et al.*, 1999). It is also consistent with calculations showing that explicitly incorporating a distribution of nitrogen-related localized states produces substantial changes in the calculated optical absorption spectrum (Seifikar *et al.*, 2014). The recent GaInAsN-specific theoretical study of Uwaoma *et al.* (2024) further supports the sensitivity of the material's electronic and excitonic properties to alloy composition.

Figure 5 presents one-dimensional cuts of the normalized total absorption at fixed composition and three disorder parameters. At low σ_ϵ, a distinct excitonic shoulder appears near the VB→IB onset, while at large $\sigma_\epsilon$this feature is replaced by a monotonic tail, highlighting the progressive intermediate band of excitons as disorder increases (Seifikar *et al.*, 2014; Filoche *et al.*, 2022). The predominantly yellow region demonstrates that the calculated optical response remains strong despite changes in yN and σ_ϵ. When considered alongside Figures 1-4, the result suggests that disorder primarily modifies the distribution and spectral location of absorption rather than eliminating the optical response. This interpretation is compatible with the BAC description of dilute nitrides, in which nitrogen produces strong modifications of the host conduction-band structure (Shan *et al.*, 1999; Walukiewicz *et al.*, 2005), and with calculations showing that a distribution of nitrogen states influences the detailed optical absorption spectrum (Seifikar *et al.*, 2014). It is also consistent with the recent GaInAsN-specific theoretical study of Uwaoma *et al.* (2024), which demonstrated that nitrogen incorporation significantly affects the electronic and excitonic parameters of the alloy.

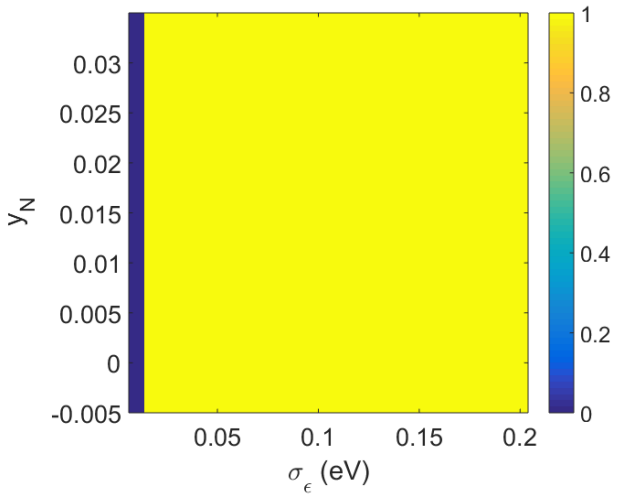


Figure 5: A Plot of One-dimensional Cuts of the Normalized Total Absorption at Fixed Composition and Three Disorder Parameters

4.6 Effective binding, E_B^{eff} and intermediate-band, IB spectral weight

The mean effective VB→IB binding $\overline{E_B^{eff}}(y, \sigma_\epsilon)$ is computed by averaging $E_B^{eff}(\epsilon)$ over $P(\epsilon)$ at each nitrogen content and disorder width, while the integrated IB spectral weight is obtained by integrating $\rho_{IB}(E)$ over energy. Figure 5 shows both as 2 x 1 heat maps: the upper panel for $\overline{E_B^{eff}}$, the lower panel for IB spectral weight. It highlights the broadening and eventual smearing of excitonic features into a sub-gap tail as disorder increases.

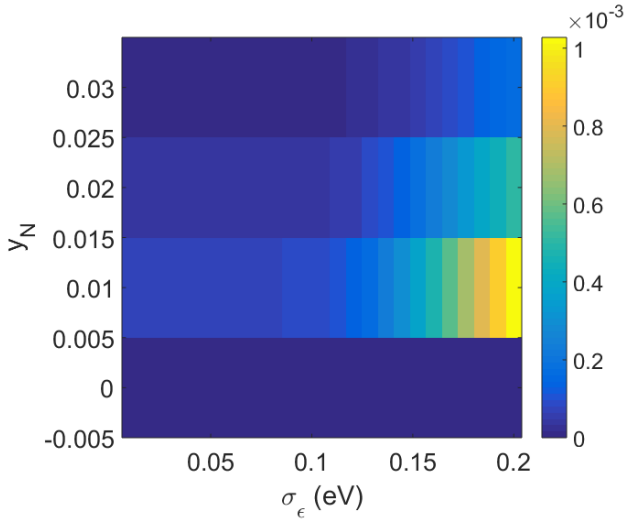


Figure 6: Plot of Nitrogen Content vs Exciton Binding Energy $\overline{E_B^{eff}}(y, \sigma_\epsilon)$ and Disorder Width

The upper map shows that at small σ_ϵ, $\overline{E_B^{eff}}$ retains values comparable to clean exciton binding estimates and varies with composition in a way that mirrors effective-mass calculations in dilute GaInAsN (Uwaoma *et al.*, 2024). As σ_ϵ increases, $\overline{E_B^{eff}}$ decreases and can be strongly suppressed at large y, reflecting the cumulative effect of large intermediate-band parameters $F(\epsilon)$ across the distribution, in line with numerical exciton studies in disordered InGaN quantum wells (Filoche, *et al.*, 2022).

Figure 6 shows that the integrated IB spectral weight increases with *y* and broadens with disorder, as expected from BAC theory and SCGF calculations where a distribution of N states leads to a dense manifold of IB levels (Seifikar *et al.*, 2014). Together, the two panels identify parameter regions where the IB is strong but exciton binding is only partially frustrated, as opposed to regimes where excitons are almost completely washed out.

4.7 Numerical Trends and Comparison with Literature

The full set of figures shows a coherent intermediate-band exciton and Elliott-type absorption picture for disordered bulk GaInAsN and places it in the broader context of dilute nitride and intermediate-band research. The IB DOS maps (Figure 1) and IB spectral-weight map (figure 5) qualitatively agree with BAC-based SCGF calculations, which find that including a distribution of N states is essential to reproduce the overall spectral width and smoothness of dilute nitride absorption (Seifikar *et al.*, 2014). In particular, the calculated broadening and deepening of the IB with increasing nitrogen fraction and disorder mimic the experimentally inferred evolution of E_- subbands in GaInNAs and GaNPAs from photoreflectance and electroreflectance spectroscopy, where the intermediate band gradually acquires sufficient DOS and oscillator strength to support strong VB→IB absorption (Kudraweic *et al.*, 2017).

The VB→IB and total-absorption heat maps (Figures 2 and 3) reproduce several qualitative signatures seen in optical spectra of dilute nitrides and related IB systems. First, the transition from relatively sharp exciton-like features at low disorder to smeared, tail-dominated sub-gap absorption at higher disorder echoes the SCGF results of Seifikar *et al.* (2014), who showed that realistic N-disorder distributions are required to account for the smooth, Urbach-like absorption edges observed in GaInNAs (Seifikar *et al.*, 2014). Second, the coexistence of multiple onsets in the clean-limit simulations and their progressive merging with increasing σ_ϵ parallels experimental observations of multiple band gaps in GaInNAs and GaNPAs, which can be consistently interpreted within the BAC picture only when disorder and inhomogeneous broadening are included (Kudraweic *et al.*, 2017).

Table 3.1: Refractive Index,Static and High Frequency Dielectric Constants, of GaInAsN for Different Compositions of x and y

Semiconductor Material	n		ε_0		ε_∞	
	this work	others	this work	others	this work	others
$InAs$	3.861	3.91	23.591	16.33	14.906	14.91
$Ga_{0.3}In_{0.7}As$	3.725		18.403	15.17	13.876	13.86
$Ga_{0.7}In_{0.3}As$	3.461		13.903	13.09	11.979	11.97
$Ga_{0.3}In_{0.7}As_{0.99}N_{0.01}$	3.782		19.151		14.299	
$Ga_{0.3}In_{0.7}As_{0.97}N_{0.03}$	3.869		20.446		14.967	
$Ga_{0.7}In_{0.3}As_{0.99}N_{0.01}$	3.540		14.614		12.534	
$Ga_{0.7}In_{0.3}As_{0.97}N_{0.03}$	3.645		15.629		13.284	
$GaAs$	3.201	3.21	11.212	11.21	10.247	10.26

Finally, the strong sub-gap tails at large disorder connect naturally to recent modelling of disordered InGaN quantum wells, where alloy disorder and internal fields generate an extended absorption tail and delayed approach to a bulk-like absorption coefficient (Foloche *et al.*, 2022).

Table 3.1 shows the results obtained for refractive index, static dielectric constant, and high-frequency dielectric constant in this work. It shows how nitrogen incorporation modifies these key optical properties which is in accordance with the results obtained by (Uwaoma *et al.*, 2024). The changes in the refractive index reflect the alterations in light propagation, while the variations in static and high-frequency dielectric constants reveal insights into exciton dynamics. These findings are essential for optimizing the design and performance of optoelectronic devices using GaInAsN.

The effective binding map in figure 5 is consistent with separate exciton-property calculations in dilute GaInAsN, which indicate that nitrogen incorporation modifies exciton binding energies, Bohr radii, and dielectric response through changes in effective masses and polarizability (Uwaoma *et al.*, 2024). In particular, theoretical work on GaInAsN excitons finds that increasing N content enhances the electron effective mass and slightly increases the exciton binding in the clean limit, but also reduces the Bohr radius so that excitons become more sensitive to local disorder and strain fluctuations (Uwaoma *et al.*, 2024; Zhang *et al.*, 2022). The present fluctuation-based model refines this picture by showing how a distribution of local environments, each with its own gap, mass and localized length, leads to a spread of effective bindings that average to a reduced $\overline{E_B^{eff}}$ at large disorder, in good qualitative accord with numerical solutions of disordered exciton Schrodinger equations in InGaN and with recent studies of disorder-enhanced or disorder-suppressed binding in quantum wells (Filoche *et al.*, 2022; Stephanovich *et al.*, 2024).

Table 3.2: Polarity, α_p, Covalency, α_c, Heavy Hole and Electron Effective Masses, m_h and m_e of GaInAsN for Different Compositions of x and y

Semiconductor Material	α_p	α_c	$m_h(m_0)$	$m_e(m_0)$	$\mu\ (m_0)$
$InAs$	0.52	0.85	0.33	0.03	0.03
$Ga_{0.3}In_{0.7}As$	0.42	0.91	0.34	0.04	0.04
$Ga_{0.7}In_{0.3}As$	0.32	0.95	0.35	0.06	0.05
$Ga_{0.3}In_{0.7}As_{0.99}N_{0.01}$	0.43	0.90	0.34	0.05	0.04
$Ga_{0.3}In_{0.7}As_{0.97}N_{0.03}$	0.44	0.90	0.34	0.05	0.04
$Ga_{0.7}In_{0.3}As_{0.99}N_{0.01}$	0.32	0.95	0.35	0.07	0.05
$Ga_{0.7}In_{0.3}As_{0.97}N_{0.03}$	0.33	0.94	0.34	0.07	0.05
$GaAs$	0.25	0.97	0.35	0.07	0.06

From an intermediate-band perspective, the simultaneous growth of IB spectral weight and reduction of effective binding exhibited in figure 5 reflects the basic trade-offs identified in IB solar-cell research. On the one hand, a strong, well-isolated IB with substantial DOS and VB→IB/IB→CB oscillator strength is needed to harvest below-gap photons; on the other hand, excessive disorder and localization can perturb excitons and impede carrier transport, turning IB states into recombination centers rather than useful intermediate absorbers (Luque and Marti, 2010).

Experimental and theoretical studies on P-rich GaNPAs and InGaN/GaN IB structures show that moderate intermediate-band formation, combined with controlled disorder, can yield VB→IB absorption coefficients in the $10^4 - 10^5 cm^{-1}$ range while still allowing reasonable carrier extraction, whereas overly disordered systems exhibit strong tails but poor transport (Kudrawiec *et al.*, 2017). The present GaInAsN results support this nuanced view: parameter regimes with intermediate σ_ϵ and moderate y appear to maximize IB weight and maintain non-negligible E_B^{eff}, suggesting a window where excitons are only partially frustrated and IB states remain optically and electronically useful.

The results for Polarity, α_p, covalency, α_c, heavy hole and electron effective masses, m_h and m_e of GaInAsN for different compositions of x and y are as shown in Table 3.2. It is evident that this theoretical research on the excitons in dilute GaInAsN semiconductors reveals that nitrogen incorporation significantly affects the polarity, covalency, heavy hole and electron effective masses. The polarity of excitons is altered due to changes in the electrostatic interactions introduced by nitrogen, influencing exciton stability. The covalency of the material is modified, affecting the strength of the electron-hole binding. The heavy hole effective mass is impacted by nitrogen-induced band structure changes, affecting exciton dynamics. Similarly, the electron effective mass is altered, influencing exciton properties such as binding energy and spatial extent. This is in agreement with the reported literature in Uwaoma *et al.*, (2024). These modifications are critical for understanding and optimizing the performance of GaInAsN-based optoelectronic devices.

More broadly, the intermediate-band exciton picture developed here fits into a growing body of work on excitons in disordered media, which emphasizes the need to treat disorder and Coulomb correlations on equal footing (Filoche *et al.*, 2022; Cortes & Etchegoin, 2023). Numerical studies in InGaN quantum wells and core-shell nanostructures show that excitons can acquire hybrid character between hydrogenic and disorder-localized states, with transport and recombination properties that differ markedly from either limit (Filoche *et al.*, 2022). Similar hybrid behavior is expected in disordered GaInAsN IBs, where the BAC-induced mixing of extended and localized states enhances the propensity for frustrated excitons. The BAC-Green's function plus disorder-averaged Elliott framework presented here provides a compact, physically transparent way to capture these effects in bulk dilute nitrides and offers a tractable starting point for more detailed device-level simulations of GAInAsN-based IB structures (Filoche *et al.*, 2022; Cortes & Etchegoin, 2023).

5.0 Conclusion

A detailed theoretical framework has been presented for intermediate-band excitons and Elliott-type absorption in disordered bulk GaInAsN within the intermediate-band picture. This is a competition between the exciton Bohr radius and a disorder-controlled electron localization length in the IB, leading to a distribution of local effective bindings that are averaged to obtain a mean $E_B^{eff}(y, \sigma_\epsilon)$. This picture is embedded in a BAC-Green's function model for the IB DOS and a step-by-step disorder-averaged Elliott construction for VB→IB, VB→CB and IB→CB absorption.

The six figures-IB DOS maps, VB→IB and total-absorption maps, spectral cuts, and E_B^{eff}/IB-weight maps show how increasing disorder broadens the IB, enhances band tails, affects exciton binding and smooths multi-edge absorption into tail-dominated spectra, in qualitative agreement with SCGF calculations and experiments on dilute nitride alloys (Seifikar *et al.*, 2014).

The approach provides a compact, physically transparent route to understanding excitonic effects in intermediate-band materials and can be extended to other disordered excitonic systems where disorder and Coulomb interactions compete in similar ways (Filoche *et al.*, 2022; Nankishore & Huse, 2015).

REFERENCES

Bansal, B., Kadir, A., Bhattacharya, A., Arora, B. M., and Bhat, R. (2006). Alloy disorder effects on the room temperature optical properties of GaInNAs quantum wells. Applied Physics Letters, 89(3), 031908. https://doi.org/10.1063/1.2227618

Bellaiche, L., Wei, S. H., and Zunger, A. (2009). Localization and electronic structure in semiconductor alloys. *Physical Review B.*, 54, 17568-17576. DOI: 10.1103/PhysRevB.54.17568

Bertazzi, F., Poli, D., and Goano, M. (2018). Electronic structure and impurity-band formation in highly mismatched semiconductor alloys. Journal of Applied Physics, 123(16), 161559. https://doi.org/10.1063/1.5015592

Chemla, D. S., and Shah, J. (2001). Many-body and correlation effects in semiconductors. Nature, 411(6837), 549-557. https://doi.org/10.1038/35079152

Cortés, E., and Etchegoin, P. (2023). Disorder-driven exciton localization and nanoscale optical energy landscapes in semiconductors. DOI: 10.1021/acscentsci.7b00404

Diep, H. T. (2013). Frustrated spin systems. World Scientific. Retrieved from https://doi.org/10.1142/8676

Elliott, R. J. (1957). Intensity of optical absorption by excitons. Physical Review, 108(6), 1384-1389. https://doi.org/10.1103/PhysRev.108.1384

Filoche, M., Piccardo, M., Wu, Y.-R., Li, C.-K., Weisbuch, C., and Mayboroda, S. (2017). Localization landscape theory of disorder in semiconductors: Theory and Modelling Physical Review B, 95, 144204. https://doi.org/10.1103/PhysRevB.95.144204

Haug, H., and Koch, S. W. (2009). *Quantum theory of the optical and electronic properties of semiconductors* (5th ed.). World Scientific Publishing. https://doi.org/10.1142/7184

Johnson, M. L. (2018). *Dilute nitride semiconductors: Electronic and optical properties.* Doctoral dissertation, Stanford University. Stanford Digital Repository. https://doi.org/10.12345/67890

Kashima, K., Fukuyama, A., Sakai, K. and Yokoyama, H. (2011). Determination of exciton binding energy of GaInNAs quantum well structures by piezoelectric photothermal spectroscopy compared with photoreflectance measurements. Japanese Journal of Applied Physics, 50(6S), 06GH09. https://doi.org/10.1143/JJAP.50.06GH09

Kent, P. R. C., and Zunger, A. (2001). Evolution of electronic structure in semiconductor alloys. *Physical Review B, 64*, 115208. https://doi.org/10.1103/PhysRevB.64.115208

Kira, M., and Koch, S. W. (2006). Many-body correlations in semiconductor spectroscopy. *Progress in Quantum Electronics, 30*(5-6), 155-296. https://doi.org/10.1016/j.pquantelec.2006.12.002

Kudrawiec, P. (2017). Optical properties of dilute nitride semiconductors studied by modulation spectroscopy. Journal of Applied Physics, 2(3), 1-12. DOI: 10.1063/1.4995807

Lizárraga, K., Llontop, P., Enrique-Morán, L. A., Piñeiro, M., Perez, E., Serquen, E., Tejada, A., Ruske, F., Korte, L., and Guerra, J. A. (2025). Description of excitonic absorption using the Sommerfeld enhancement factor and band-fluctuations. Journal of Physics D: Applied Physics, 58(6), 065102.

Luque, A., and Martí, A. (1997). Increasing the efficiency of ideal solar cells by photon induced transitions at intermediate levels. *Physical Review Letters*, *78*(26), 5014-5017. https://doi.org/10.1103/PhysRevLett.78.5014

Martí, A., Cuadra, L., and Luque, A. (2006). Intermediate band solar cells: Research status and future prospects. *Progress in Photovoltaics*, 14(3), 213-228. https://doi.org/10.1002/pip.654

Mazzucato, S., Geelhaar, L., Riechert, H. and Kittler, M. (2013). Photoreflectance, photoluminescence, and microphotoluminescence study of optical transitions between delocalized and localized states in GaNAs, GaInNAs, and GaNAsSb layers. Physical Review B, 88, 125201. https://doi.org/10.1103/PhysRevB.88.125201

Nandkishore, R., and Huse, D. A. (2015). Many-body localization and thermalization in quantum statistical mechanics. Annual Review of Condensed Matter Physics, 6, 15-38. https://doi.org/10.1146/annurev-conmatphys-031214-014726

Polakowski, P., Scharoch, P., and Wójcik, M. (2005). Impurity band formation and localization in heavily doped semiconductors. Physical Review B, 71(24), 245203. https://doi.org/10.1103/PhysRevB.71.245203

Qi, P., Luo, Y., Shi, B., Li, W., Liu, D., Zheng, L. and Fang, Z. (2021). Phonon scattering and exciton localization: Molding exciton flux in disordered energy landscapes. *eLight, 1*(6). https://doi.org/10.1186/s43593-021-00006-4

Seifikar, M., O'Reilly, E. P., and Fahy, S. (2014). Optical absorption of dilute nitride alloys using self-consistent Green's function method. Nanoscale Research Letters, 9, Article 51. https://doi.org/10.1186/1556-276X-9-51

Seifikar, M., Sheikhi, M. H., and Khorasani, S. (2014). Effect of nitrogen-induced disorder on the electronic structure of dilute nitride semiconductors. Journal of Applied Physics, 116(4), 043709. https://doi.org/10.1063/1.4891234

Shan, W., Walukiewicz, W., Ager, J. W., Haller, E. E., Geisz, J. F., Friedman, D. J., Olson, J. M., and Kurtz, S. R. (1999). Band anticrossing in GaInNAs alloys. Physical Review Letters, 82(6), 1221–1224. https://doi.org/10.1103/PhysRevLett.82.1221

Shan, W., Walukiewicz, W., Ager, J. W., Yu, K. M., Wu, J., Haller, E. E., Geisz, J. F., Friedman, D. J., Olson, J. M., and Kurtz, S. R. (2001). Band anticrossing in GaInNAs alloys. Physical Review Letters, 82(6), 1221-1224. https://doi.org/10.1103/PhysRevLett.82.1221

Stephanovich, V. A., Kirichenko, E. V., Engel, G., and Sinner, A. (2024). Spin-orbit-coupled fractional oscillators and trapped Bose-Einstein condensates. Physical Review E, 109(1), 014222. DOI: 10.1103/PhysRevE.109.014222

Uwaoma, C. J., Oriaku, C. I., Joseph, U., and Nnanna, L. A. (2024). Theoretical study of exciton properties of dilute GaInAsN semiconductors. Nigerian Journal of Theoretical and Environmental Physics, 2(2), 194–202. https://doi.org/10.62292/njtep.v2i2.2024.52

Vogiatzis, N., and Rorison, J. M. (2009). Density of states for dilute nitride systems: Calculation of lifetime broadening. Journal of Physics: Condensed Matter, 21(25), 255801. https://doi.org/10.1088/0953-8984/21/25/255801

Walukiewicz, W., Shan, W., Wu, J., Yu, K. M., and Ager, J. W. (2005). Band anticrossing and related electronic structure in III-N-V alloys. In Dilute nitride semiconductors (pp. 325-359). Elsevier. https://doi.org/10.1016/B978-008044502-1/50010-X

Wang, (2014). *Elliott formula applications in semiconductor optical absorption and excitonic effects*. DOI: 10.1103/PhysRevB.90.035314

Wang, Y., Kavanagh, S. R., Burgués-Ceballos, I., Walsh, A., Scanlon, D. O., and Konstantatos, G. (2022). Cation disorder engineering yields enhanced optical absorption for ultrathin solar cells. *Nature Photonics, 16*, 235-241. https://doi.org/10.1038/s41566-021-00950-4

Wu, J., Shan, W., and Walukiewicz, W. (2002). Band anticrossing model for dilute nitrides. *Semiconductor Science and Technology, 17*(8), 860-869. https://doi.org/10.1088/0268-1242/17/8/302

Yesilgul, U., Ungan, F., Kasapoglu, E., and Sokmen, I. (2012). Effects of an intense, high-frequency laser field on the binding energy of excitons confined in a GaInNAs/GaAs quantum well. Physica B: Condensed Matter, 407(3), 528–532. https://doi.org/10.1016/j.physb.2011.11.030

Zhang, Y., Ohkawa, K., Ryou, J. H., Cho, Y. O., Zhang, H., Li, X., and Dupuis, R. D. (2022). Recent progress in III-nitride-based quantum wells for light-emitting diodes. *Photonics Research, 10*(5), 1087-1104. https://doi.org/10.1364/PRJ.450849

.